Journal of Alloys and Compounds 499 (2010) 108–112

Contents lists available at ScienceDirect

Journal of Alloys and Compounds

journal homepage: www.elsevier.com/locate/jallcom

The magnetic properties of La doped and codoped $BiFeO_3$

Xiaohong Zheng[a], Qingyu Xu[a,*], Zheng Wen[b], Xianzhong Lang[a], D. Wu[b], T. Qiu[a], M.X. Xu[a]

[a] Department of Physics, Southeast University, Nanjing 211189, China
[b] Department of Materials Science and Engineering, Nanjing University, Nanjing 210008, China

ARTICLE INFO

Article history:
Received 3 March 2010
Received in revised form 10 March 2010
Accepted 13 March 2010
Available online 18 March 2010

PACS:
75.85.+t
75.50.Dd
78.30.Am

Keywords:
Multiferroic
Ferromagnetism
Raman

ABSTRACT

La doped $BiFeO_3$, $Bi(Fe_{0.95}Co_{0.05})O_3$ and $Bi(Fe_{0.95}Mn_{0.05})O_3$ ceramics have been prepared by sol–gel method with rapid sintering process. X-ray diffraction spectra show that the impurity phase has been effectively suppressed by La doping. The magnetic measurements show that 10% La doping on Bi sites has little influence on the magnetic properties of $BiFeO_3$ and $Bi(Fe_{0.95}Co_{0.05})O_3$, while significantly enhances the magnetization of $Bi(Fe_{0.95}Mn_{0.05})O_3$. Raman measurements show larger structure distortion by Co doping or La and Mn codoping on $BiFeO_3$, which explains the significant enhancement of magnetization. Our results suggest that small amount of La doping can be an effective way to prepare high quality $BiFeO_3$ and its derivatives.

1. Introduction

Multiferroic materials have attracted much attention due to their multifunctional properties [1]. These materials posses the magnetoelectric effect (ME) which allows the coupling between polarization and magnetization, making them promising candidates for applications in memories, spintronics and magnetoelectric sensor devices [2,3]. Among the rare multiferroic materials, $BiFeO_3$ is one of the well-know single-phase multiferroic materials with G-type antiferromagnetic behavior below Neel temperature $T_N \sim 643$ K and ferroelectric behavior below Curie temperature $T_c \sim 1103$ K [4]. $BiFeO_3$ has a superimposed incommensurate cycloid spin structure with a periodicity of about 64 nm [5]. This structure cancels the macroscopic magnetization and inhibits the observation of the linear ME effect [6]. The decrease in particle size has been proven to be effective in suppressing the cycloid structure and enhancing the magnetic moment of $BiFeO_3$ [7,8]. Ion substitution is an alternative effective method to enhance the magnetization in $BiFeO_3$. Sr, Ba, etc. were used to partially substitute Bi, and Co, Ni, etc. were used to partially substitute Fe, which significantly enhanced the room temperature ferromagnetism [9–11]. The enhanced ferromagnetism may make $BiFeO_3$ possible be used in tunnel junctions as a multiferroic spin filtering barrier [12].

However, it is difficult to synthesis single-phase $BiFeO_3$ bulk ceramics. Impurity phases, such as $Bi_2Fe_4O_9$, $Bi_{25}FeO_{39}$ can always be observed [11,13]. Generally the impurity phase was always removed by leaching in diluted HNO_3 [13]. In this paper, we study the structure and magnetic properties of La doped and codoped $BiFeO_3$. La has been confirmed to be an effective dopant to suppress the impurity phase in $BiFeO_3$ and its derivatives. Furthermore, La doping has little influence on the magnetic properties, except for the enhancement of magnetization in La doped Bi $(Fe_{0.95}Mn_{0.05})O_3$.

2. Experimental

$BiFeO_3$, $(Bi_{0.9}La_{0.1})FeO_3$, $Bi(Fe_{0.95}Co_{0.05})O_3$, $(Bi_{0.9}La_{0.1})(Fe_{0.95}Co_{0.05})O_3$, $Bi(Fe_{0.95}Mn_{0.05})O_3$ and $(Bi_{0.9}La_{0.1})(Fe_{0.95}Mn_{0.05})O_3$ ceramics were prepared by sol–gel method with rapid sintering process. Appropriate amounts of $Bi(NO_3)_3{\cdot}5H_2O$, $Fe(NO_3)_3{\cdot}9H_2O$, $Co(NO_3)_2{\cdot}6H_2O$, $Mn(NO_3)_2$ and $La(NO_3)_3{\cdot}nH_2O$ were dissolved in ethylene glycol. The obtained solutions were dried at 80 °C, and then calcined at 450 °C in air for 24 h. The obtained powders were grinded, and pressed into 1 mm thick disks in diameter of 13 mm. The disks were directly put into an 800 °C oven and sintered in air for 20 min. The sintered disks were taken out from the oven and cooled to room temperature within several minutes. The structures of samples were studied by X-ray diffraction (XRD) with Cu Kα radiation and scanning electron microscope (SEM). Raman measurements were carried out on a Horiba Jobin Yvon LabRAM HR 800 micro-Raman spectrometer with 785 nm excitation source under air ambient condition at room

* Corresponding author. Tel.: +86 2552090600x8308; fax: +86 2552090600x8204.
E-mail address: xuqingyu@seu.edu.cn (Q. Xu).

0925-8388/$ – see front matter © 2010 Elsevier B.V. All rights reserved.
doi:10.1016/j.jallcom.2010.03.131

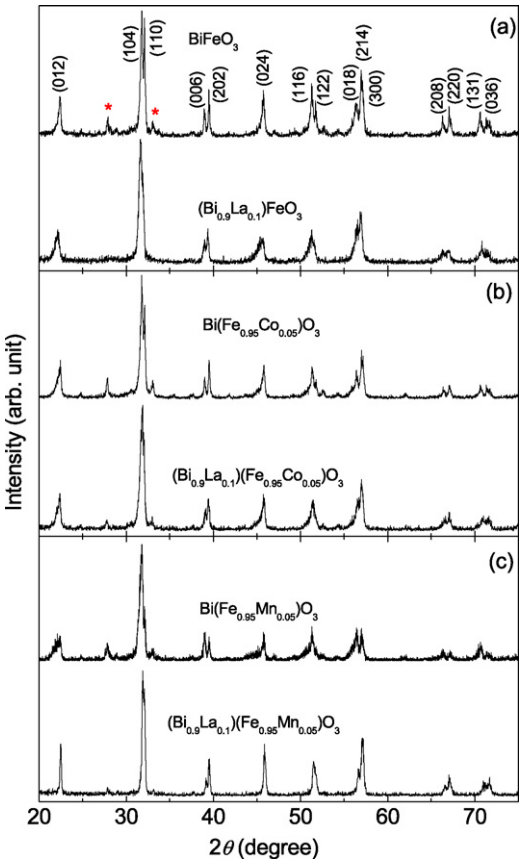

Fig. 1. XRD patterns of (a) $BiFeO_3$ and $(Bi_{0.9}La_{0.1})FeO_3$, (b) $Bi(Fe_{0.95}Co_{0.05})O_3$ and $(Bi_{0.9}La_{0.1})(Fe_{0.95}Co_{0.05})O_3$, (c) $Bi(Fe_{0.95}Mn_{0.05})O_3$ and $(Bi_{0.9}La_{0.1})(Fe_{0.95}Mn_{0.05})O_3$. The stars mark the impurity phase of $Bi_{25}FeO_{39}$.

temperature. The laser focused on the sample surface in diameter of 1 μm. The magnetization of the samples was measured by a vibrating sample magnetometer integrated in a physical property measurement system (PPMS-9, Quantum Design).

3. Results and discussions

The XRD patterns of the sintered $BiFeO_3$, $(Bi_{0.9}La_{0.1})FeO_3$, $Bi(Fe_{0.95}Co_{0.05})O_3$, $(Bi_{0.9}La_{0.1})(Fe_{0.95}Co_{0.05})O_3$, $Bi(Fe_{0.95}Mn_{0.05})O_3$ and $(Bi_{0.9}La_{0.1})(Fe_{0.95}Mn_{0.05})O_3$ ceramics are shown in Fig. 1. It can be seen that all specimens mainly exhibit the rhombohedral structure (*R*3*c*). In Fig. 1(a), small impurity peaks marked by stars at 2θ around 30° have been observed in $BiFeO_3$, which correspond to $Bi_{25}FeO_{39}$. The impurity phase of $Bi_{25}FeO_{39}$ can also be observed in $Bi(Fe_{0.95}Co_{0.05})O_3$ and $Bi(Fe_{0.95}Mn_{0.05})O_3$, as shown in Fig. 1(b) and (c). With 10% La substituting Bi in $BiFeO_3$, no trace of $Bi_{25}FeO_{39}$ has been observed. $(Bi_{0.9}La_{0.1})FeO_3$ exhibits pure *R*3*c* structure. Though $Bi_{25}FeO_{39}$ can still be observed in $(Bi_{0.9}La_{0.1})(Fe_{0.95}Co_{0.05})O_3$ and $(Bi_{0.9}La_{0.1})(Fe_{0.95}Mn_{0.05})O_3$, but the intensity of the diffraction peaks is much weaker. This suggests that the impurity phase has been effectively suppressed with 10% La doping. The lattice constants *a* and *c* can be calculated from the XRD patterns ($a = 5.571$ Å and $c = 13.873$ Å for $BiFeO_3$, $a = 5.578$ Å and $c = 13.839$ Å for $(Bi_{0.9}La_{0.1})FeO_3$, $a = 5.576$ Å and $c = 13.839$ Å for $Bi(Fe_{0.95}Co_{0.05})O_3$, $a = 5.576$ Å and $c = 13.805$ Å for $(Bi_{0.9}La_{0.1})(Fe_{0.95}Co_{0.05})O_3$, $a = 5.582$ Å and $c = 13.832$ Å for $Bi(Fe_{0.95}Mn_{0.05})O_3$, $a = 5.569$ Å and $c = 13.791$ Å for $(Bi_{0.9}La_{0.1})(Fe_{0.95}Mn_{0.05})O_3$). *a* keeps constant and *c* decreases for 10% La doped $BiFeO_3$ and $Bi(Fe_{0.95}Co_{0.05})O_3$, while *a* and *c* both decrease for 10% La doped $Bi(Fe_{0.95}Mn_{0.05})O_3$.

Fig. 2 shows the typical surface SEM images of $BiFeO_3$, $(Bi_{0.9}La_{0.1})FeO_3$, $Bi(Fe_{0.95}Co_{0.05})O_3$, $(Bi_{0.9}La_{0.1})(Fe_{0.95}Co_{0.05})O_3$, $Bi(Fe_{0.95}Mn_{0.05})O_3$ and $(Bi_{0.9}La_{0.1})(Fe_{0.95}Mn_{0.05})O_3$ ceramics. La doping did not exhibit systematic influence on the grain size. The grain size of $BiFeO_3$ is rather nonuniform and estimated to be about 1–2 μm. With 10% La substitution, the grain size is more uniform and increases slightly. However, for $Bi(Fe_{0.95}Co_{0.05})O_3$, the grain size decreases with 10% La doping. The grain size changes little after 10% La doping for $Bi(Fe_{0.95}Mn_{0.05})O_3$.

Details of the structure evolution with ion substitution on $BiFeO_3$ can be expressed more explicitly through Raman spectra [14]. The Raman spectra of samples are shown in Fig. 3. The clearly resolved Raman modes of the samples are marked by arrows in Fig. 3, which can all be indexed to the modes of $BiFeO_3$ molecule [15,16]. As the intensity of the Raman peaks of $BiFeO_3$ decrease with increasing temperature, not all modes can be clearly observed above room temperature [17]. We concentrate here on those peaks which can be clearly resolved in the spectra. The peak position was determined by the Gaussian fit, and listed in Table 1. Compared with the peak positions of $BiFeO_3$, all the Raman peaks of $Bi(Fe_{0.95}Co_{0.05})O_3$ shift to lower frequencies. Less change can be observed on $Bi(Fe_{0.95}Mn_{0.05})O_3$. The E-1 mode associates with Bi ions and A_1-1 mode associates with Fe ions [18,19]. The larger shift of the A_1-1 mode of $Bi(Fe_{0.95}Co_{0.05})O_3$ to lower frequency shows that Co doping produces more structural distortion on Fe site. Interestingly, though less shift of A_1-1 mode in $Bi(Fe_{0.95}Mn_{0.05})O_3$ is observed, greater shift has been observed on $(Bi_{0.9}La_{0.1})(Fe_{0.95}Mn_{0.05})O_3$, indicating that 10% La doping produces significant structure distortion on Fe site. No shift of the A_1-1 mode is observed on $(Bi_{0.9}La_{0.1})(Fe_{0.95}Co_{0.05})O_3$ compared with $Bi(Fe_{0.95}Co_{0.05})O_3$. Higher frequency Raman modes are generally associated with vibrational modes involving oxygen [19]. As can be clearly seen in Table 1, the E-3 mode of $Bi(Fe_{0.95}Co_{0.05})O_3$ shows greater shift to lower frequency than that of $Bi(Fe_{0.95}Mn_{0.05})O_3$, indicating the more rotation of the oxygen octahedral associated with the *R*3*c* space group [19]. Similar to A_1-1 mode, significant shift to lower frequency is observed on $(Bi_{0.9}La_{0.1})(Fe_{0.95}Mn_{0.05})O_3$, indicating La doping on $Bi(Fe_{0.95}Mn_{0.05})O_3$ induces more rotation of the oxygen octahedral.

Table 1
Raman modes of $BiFeO_3$, $Bi(Fe_{0.95}Co_{0.05})O_3$, $Bi(Fe_{0.95}Mn_{0.05})O_3$, $(Bi_{0.9}La_{0.1})FeO_3$, $(Bi_{0.9}La_{0.1})(Fe_{0.95}Co_{0.05})O_3$, and $(Bi_{0.9}La_{0.1})(Fe_{0.95}Mn_{0.05})O_3$ ceramics.

Modes	E-1 (cm^{-1})	A_1-1 (cm^{-1})	A_1-2 (cm^{-1})	E-3 (cm^{-1})	E-7 (cm^{-1})	E-8 (cm^{-1})	E-9 (cm^{-1})
$BiFeO_3$	73	137	171	274		522	619
B $(Fe_{0.95}Co_{0.05})O_3$	72	133	168	268	477		610
B $(Fe_{0.95}Mn_{0.05})O_3$	71	136	170	275			622
$(Bi_{0.9}La_{0.1})FeO_3$	71	139	172	274	481	527	625
$(Bi_{0.9}La_{0.1})(Fe_{0.95}Co_{0.05})O_3$	69	133	167	271	474	529	616
$(Bi_{0.9}La_{0.1})(Fe_{0.95}Mn_{0.05})O_3$	70	134	170	267	477		625

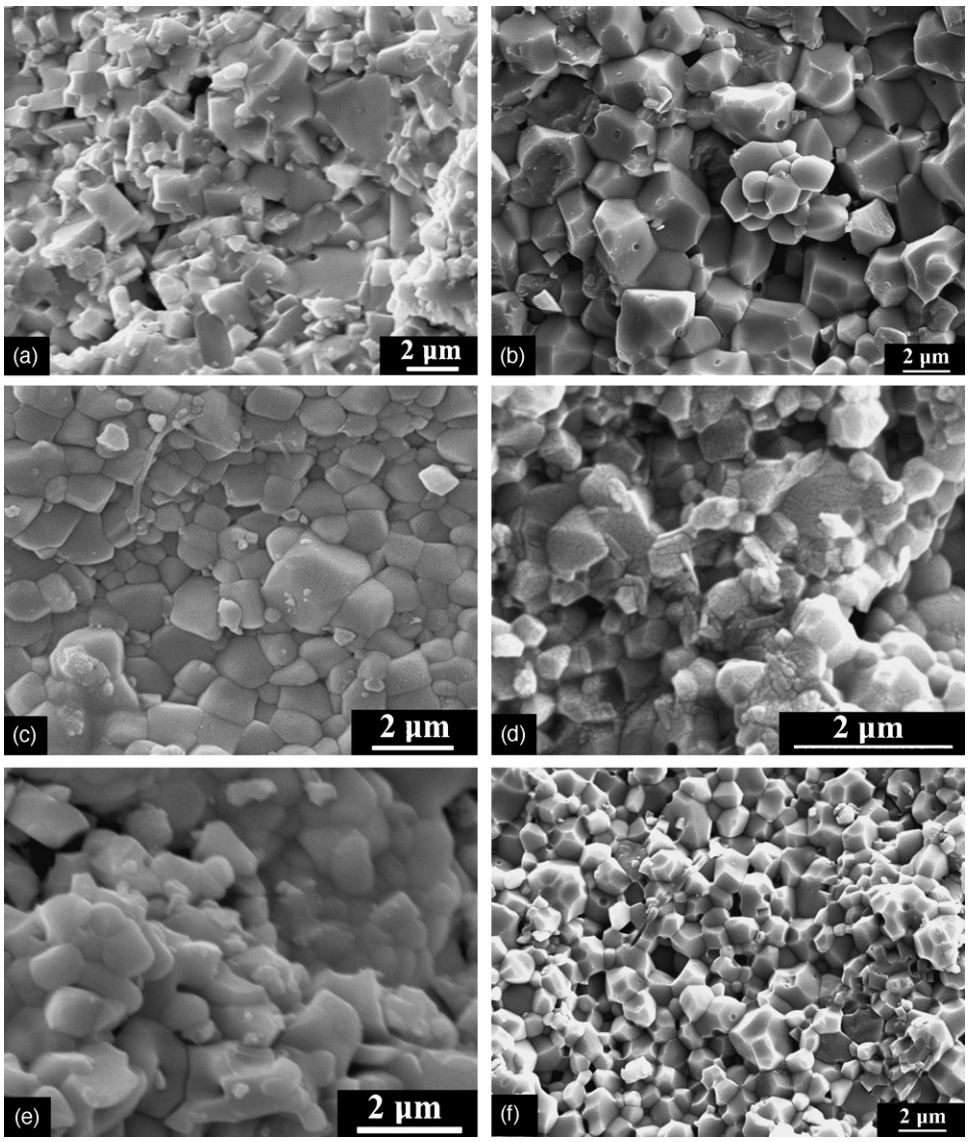

Fig. 2. Surface SEM images of (a) $BiFeO_3$, (b) $(Bi_{0.9}La_{0.1})FeO_3$, (c) $Bi(Fe_{0.95}Co_{0.05})O_3$, (d) $(Bi_{0.9}La_{0.1})(Fe_{0.95}Co_{0.05})O_3$, (e) $Bi(Fe_{0.95}Mn_{0.05})O_3$, and (f) $(Bi_{0.9}La_{0.1})(Fe_{0.95}Mn_{0.05})O_3$.

Fig. 4 shows the room temperature magnetization hysteresis loops for $BiFeO_3$, $(Bi_{0.9}La_{0.1})FeO_3$, $Bi(Fe_{0.95}Co_{0.05})O_3$, $(Bi_{0.9}La_{0.1})(Fe_{0.95}Co_{0.05})O_3$, $Bi(Fe_{0.95}Mn_{0.05})O_3$ and $(Bi_{0.9}La_{0.1})(Fe_{0.95}Mn_{0.05})O_3$ ceramics. $BiFeO_3$ exhibits weak ferromagnetism, which is due to the induced lattice distortion by the rapid sintering and fast cooling process [20]. The high field linear *M–H* curve is commonly observed in bulk $BiFeO_3$ which is due to the antiferromagnetic arrangement of Fe^{3+} spins. $Bi(Fe_{0.95}Co_{0.05})O_3$ exhibits enhanced ferromagnetism with clear hysteresis loop, and the magnetization is about 2 orders larger than that of $BiFeO_3$. The magnetization of $Bi(Fe_{0.95}Mn_{0.05})O_3$ is almost the same as that of $BiFeO_3$, though the coercivity is increased significantly. Compared with the magnetization of their parent materials, the magnetization of $BiFeO_3$ and $Bi(Fe_{0.95}Co_{0.05})O_3$ keeps almost constant, but the magnetization of $(Bi_{0.9}La_{0.1})(Fe_{0.95}Mn_{0.05})O_3$ is one order larger with 10% La doping. Interestingly, $(Bi_{0.9}La_{0.1})(Fe_{0.95}Mn_{0.05})O_3$ exhibits a second jump of magnetization at about 2500 Oe, which has been observed in $Bi(Fe_{0.95}Co_{0.05})O_3$ at low temperatures [11]. At this moment, we are still not clear about the origin of this double-loop hysteresis. We suggested that it might originate from the ferrimagnetic interaction between Mn and Fe ions due to the incorporation of La ions [11].

Raman results have shown that Co doping induced significant structure distortion in $BiFeO_3$ but Mn doping has little influence. Khomchenko et al. have found that larger magnetization can be achieved by substituting with the ions of larger radius. The larger ions can induce larger structure distortion and suppress the spiral spin configuration [10]. Thus $Bi(Fe_{0.95}Co_{0.05})O_3$ exhibits enhanced magnetization of 2 orders larger than that of $BiFeO_3$, and the magnetization of $Bi(Fe_{0.95}Mn_{0.05})O_3$ is almost the same as that of $BiFeO_3$. Compared with their parent materials, $(Bi_{0.9}La_{0.1})FeO_3$ and $(Bi_{0.9}La_{0.1})(Fe_{0.95}Co_{0.05})O_3$ show less structure distortion while significant structure distortion has been observed on $(Bi_{0.9}La_{0.1})(Fe_{0.95}Mn_{0.05})O_3$. Thus $(Bi_{0.9}La_{0.1})FeO_3$ and $(Bi_{0.9}La_{0.1})(Fe_{0.95}Co_{0.05})O_3$ exhibit similar magnetic properties as $BiFeO_3$ and $Bi(Fe_{0.95}Co_{0.05})O_3$, respectively. The magnetization of $(Bi_{0.9}La_{0.1})(Fe_{0.95}Mn_{0.05})O_3$ is significantly enhanced compared with $Bi(Fe_{0.95}Mn_{0.05})O_3$.

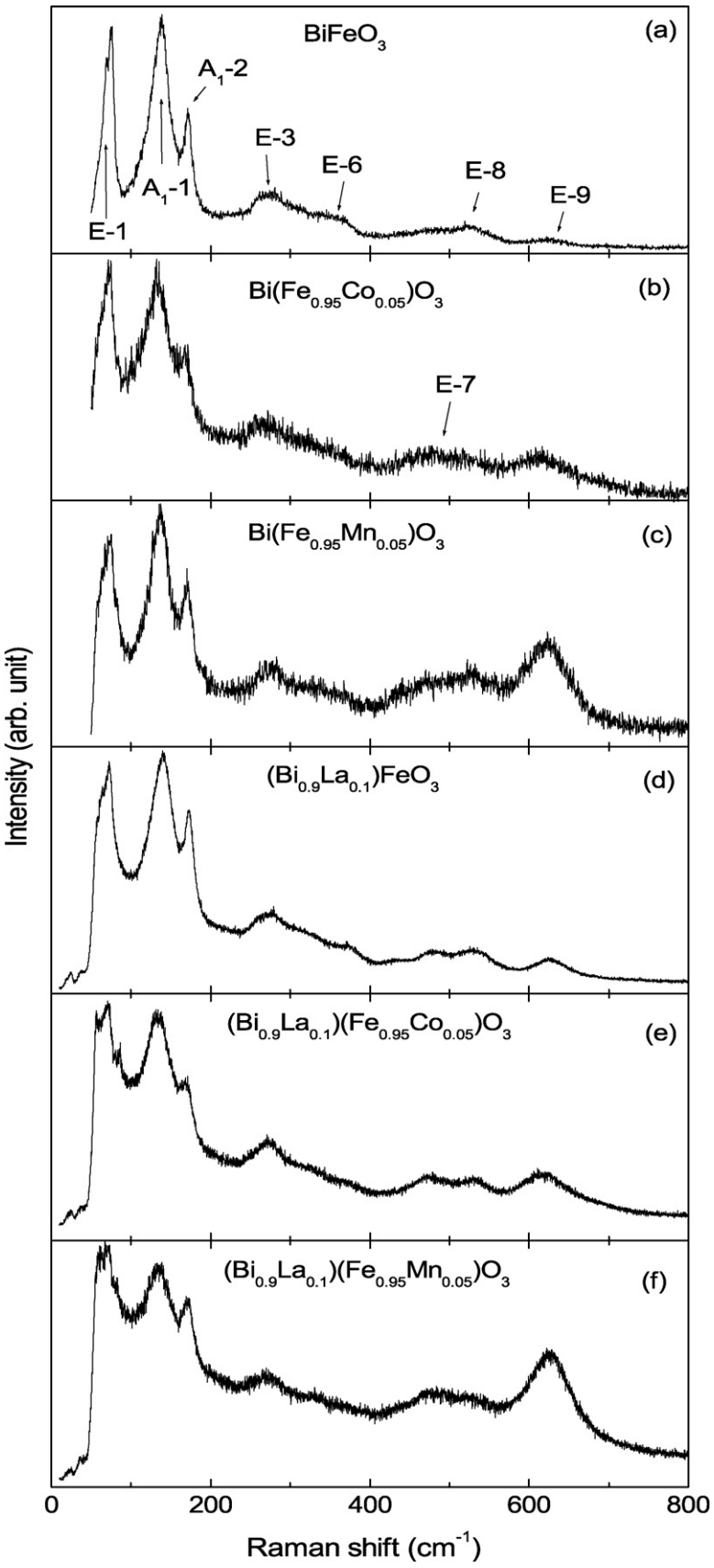

Fig. 3. Room temperature Raman spectra of (a) $BiFeO_3$, (b) $Bi(Fe_{0.95}Co_{0.05})O_3$, (c) $Bi(Fe_{0.95}Mn_{0.05})O_3$, (d) $(Bi_{0.9}La_{0.1})FeO_3$, (e) $(Bi_{0.9}La_{0.1})(Fe_{0.95}Co_{0.05})O_3$, and (f) $(Bi_{0.9}La_{0.1})(Fe_{0.95}Mn_{0.05})O_3$.

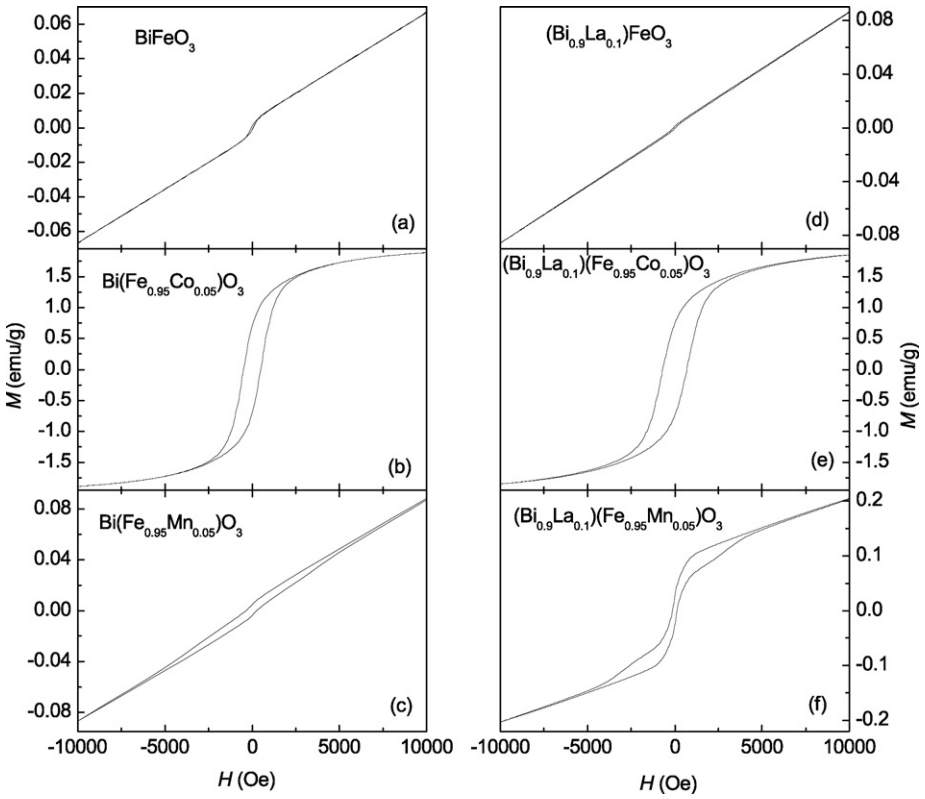

Fig. 4. Magnetic hysteresis loops measured at 300 K of (a) $BiFeO_3$, (b) $Bi(Fe_{0.95}Co_{0.05})O_3$, (c) $Bi(Fe_{0.95}Mn_{0.05})O_3$, (d) $(Bi_{0.9}La_{0.1})FeO_3$, (e) $(Bi_{0.9}La_{0.1})(Fe_{0.95}Co_{0.05})O_3$, and (f) $(Bi_{0.9}La_{0.1})(Fe_{0.95}Mn_{0.05})O_3$.

4. Conclusions

10% La has been doped into $BiFeO_3$, $Bi(Fe_{0.95}Co_{0.05})O_3$ and $Bi(Fe_{0.95}Mn_{0.05})O_3$ ceramics. The impurity phase was effective suppressed, which is confirmed from XRD measurements. Raman measurements show clearly the larger structure distortion by Co doping on $BiFeO_3$ and La doping on $Bi(Fe_{0.95}Mn_{0.05})O_3$. The magnetic measurements show that 10% La doping on Bi sites has little influence on the magnetic properties of $BiFeO_3$ and $Bi(Fe_{0.95}Co_{0.05})O_3$, while significantly enhances the magnetization of $Bi(Fe_{0.95}Mn_{0.05})O_3$. Our work confirms that the enhanced magnetization is due to the larger structure distortion which suppresses the spiral spin configuration.

Acknowledgments

This work is supported by the National Natural Science Foundation of China (50802041, 50872050), National Key Projects for Basic Researches of China (2010CB923404, 2009CB929503) and Southeast University. M.X. Xu acknowledges the support from the Research Fund for the Doctoral Program of Higher Education of China (Grant No. 20070286037).

References

[1] K.F. Wang, J.M. Liu, Z.F. Ren, Adv. Phys. 58 (2009) 321–448.
[2] J. Wang, J.B. Neaton, H. Zheng, V. Nagarajan, S.B. Ogale, B. Liu, D. Viehland, V. Vaithyanathan, D.G. Schlom, U.V. Waghmare, N.A. Spaldin, K.M. Rabe, M. Wuttig, R. Ramesh, Science 299 (2003) 1719–1722.
[3] N. Hur, S. Park, P.A. Sharma, J.S. Ahn, S. Guha, S.-W. Cheong, Nature 429 (2004) 392–395.
[4] G. Catalan, J.F. Scott, Adv. Mater. 21 (2009) 2463–2485.
[5] D. Lebeugle, D. Colson, A. Forget, M. Viret, A.M. Bataille, A. Gukasov, Phys. Rev. Lett. 100 (2008) 227602.
[6] H. Béa, M. Bibes, S. Petit, J. Kreisel, A. Barthélémy, Phil. Mag. Lett. 87 (2007) 165–174.
[7] S. Vijayanand, M.B. Mahajan, H.S. Potdar, P.A. Joy, Phys. Rev. B 80 (2009) 064423.
[8] T. Park, G.C. Papaefthymiou, A.J. Viescas, A.R. Moodenbough, S.S. Wong, Nano Lett. 7 (2007) 766–772.
[9] V.B. Naik, R. Mahendiran, Solid State Commun. 149 (2009) 754–758.
[10] V.A. Khomchenko, D.A. Kiselev, M. Kopcewicz, M. Maglione, V.V. Shvartsman, P. Borisov, W. Kleemann, A.M.L. Lopes, Y.G. Pogorelov, J.P. Araujo, R.M. Rubinger, N.A. Sobolev, J.M. Vieira, A.L. Kholkin, J. Magn. Magn. Mater. 321 (2009) 1692–1698.
[11] Q. Xu, H. Zai, D. Wu, T. Qiu, M.X. Xu, Appl. Phys. Lett. 95 (2009) 112510.
[12] M. Gajek, M. Bibes, S. Fusil, K. Bouzehouane, J. Fontcuberta, A. Barthélémy, A. Fert, Nat. Mater. 6 (2007) 296–302.
[13] D. Lebeugle, D. Colson, A. Forget, M. Viret, P. Bonville, J.F. Marucco, S. Fusil, Phys. Rev. B 76 (2007) 024116.
[14] Y. Wang, C. Nan, J. Appl. Phys. 103 (2008) 114104.
[15] P. Hermet, M. Goffinet, J. Kreisel, Ph. Ghosez, Phys. Rev. B 75 (2007) 220102.
[16] Y. Yang, J.Y. Sun, K. Zhu, Y.L. Liu, L. Wan, J. Appl. Phys. 103 (2008) 093532.
[17] D. Rout, K. Moon, S.L. Kang, J. Raman Spectrosc. 40 (2009) 618–626.
[18] S. Yasui, H. Uchida, H. Nakaki, K. Nishida, H. Funakubo, S. Koda, Appl. Phys. Lett. 91 (2007) 022906.
[19] P. Kharel, S. Talebi, B. Ramachandran, A. Dixit, V.M. Naik, M.B. Sahana, C. Sudakar, R. Naik, M.S.R. Rao, G. Lawes, J. Phys.: Condens. Matter 21 (2009) 036001.
[20] Q. Xu, H. Zai, D. Wu, Y.K. Tang, M.X. Xu, J. Alloys Compd. 485 (2009) 13–16.